

# Temperature dependent properties of spray deposited $\text{Cu}_2\text{CoSnS}_4$ (CCTS) thin films

P. S. Maldar<sup>1</sup> · A. A. Mane<sup>1</sup> · S. S. Nikam<sup>1</sup> · S. D. Giri<sup>2</sup> · A. Sarkar<sup>2</sup> · A. V. Moholkar<sup>1</sup>

Received: 28 May 2017 / Accepted: 31 August 2017 / Published online: 8 September 2017  
© Springer Science+Business Media, LLC 2017

**Abstract** A modified spray pyrolysis technique was employed for the deposition of  $\text{Cu}_2\text{CoSnS}_4$  (CCTS) thin films. X-ray diffraction study showed that the CCTS thin films exhibit stannite structure with preferred orientation along (112) plane. The phase purity of sprayed CCTS films was confirmed from Raman analysis, as the most intense peak is observed at  $320\text{ cm}^{-1}$  corresponding to A1 mode. With increase in substrate temperature the grains over the surface of the CCTS films become more distinct. The EDAX spectrum revealed the presence of different constituent elements such as, Cu, Co, Sn and S for the films deposited at  $325\text{ }^\circ\text{C}$ . The optical absorption study showed that the energy band gap values of the CCTS films are decreasing from 1.70 to 1.46 eV with respect to increase in substrate temperature from 275 to  $325\text{ }^\circ\text{C}$ .

## 1 Introduction

In order to fulfill the demand for green energy through photovoltaics much emphasis is needed in the development of new materials which can harvest solar energy for electricity generation [1]. The development of cost effective thin film solar cells (TFSC) based on nontoxic, and earth abundant materials, requires the exploration of new photoactive materials.  $\text{Cu}_2\text{CoSnS}_4$  (CCTS) is a compound semiconductor, with optimal band gap value in the range 1.46–1.61 eV,

which suggest its high potential application in the photovoltaic field for the development of efficient TFSC. In addition, it offers direct band gap that reduces the material need in comparison to other indirect band gap materials like crystalline silicon [2]. CCTS has stannite structure which crystallizes in the tetragonal space group  $I\bar{4}2m$ . In the tetragonal unit cell all three metal atoms are tetrahedrally surrounded by sulfur atom, and each sulfur atom is surrounded by one Co, one Sn, and two Cu atoms [3]. In stannite structure, Co and Sn atoms are in the same layer alter their positions every other layer. A layer of Cu alternates with a layer of Co and Sn [4]. The CCTS semiconductor has been synthesised by different techniques such as, hydrothermal [5], solvothermal [6–8], sol–gel [9], hot injection [10], solid state reaction [11] electrospinning [12–14], high temperature route [15, 16], melt and anneal process [17, 18]. The most of the research in case of CCTS has been devoted in the synthesis of nanocrystals. With an intention of practical application in photovoltaic devices, the CCTS thin films need to be thoroughly studied. Among the diverse methods available for synthesis of thin films the spray pyrolysis technique offers certain advantages such as easy handling, non vacuum and large area deposition [19].

This paper represents effect of temperature on structural, morphological and optical properties of spray deposited CCTS thin films. The CCTS thin films are deposited with PID logic using Arduino platform. The working temperature range is maintained with precision of  $(\pm 2)\text{ }^\circ\text{C}$  related to operating temperature set by user. The Arduino platform is also utilized to drive DC motor which provides mechanized movement of the spray nozzle to facilitate the regular deposition of thin films.

✉ A. V. Moholkar  
avmoholkar@gmail.com

<sup>1</sup> Thin Film Nano-materials Laboratory, Department of Physics, Shivaji University, Kolhapur 416-004, India

<sup>2</sup> Department of Chemical Engineering, Indian Institute of Technology Bombay, Powai, Mumbai 400076, India

## 2 Experimental details

Figure 1 shows the schematic of the spray pyrolysis unit used for deposition of CCTS thin films. The deposition of CCTS thin films was carried out using precursors, 0.05 M  $\text{CuCl}_2 \cdot 2\text{H}_2\text{O}$  (Cupric Chloride) for copper, 0.025 M  $\text{CoCl}_2 \cdot 6\text{H}_2\text{O}$  (Cobalt Chloride hexahydrate) for cobalt, 0.025 M  $\text{SnCl}_4 \cdot 5\text{H}_2\text{O}$  (Stannic Chloride) for tin, and thiourea ( $\text{CH}_4\text{N}_2\text{S}$ ) was used in excess than stoichiometry as a source of sulfur. Methanol was used as solvent to prepare precursor solution. The 0.05 M  $\text{CuCl}_2 \cdot 2\text{H}_2\text{O}$  solution was prepared by dissolving 0.17 g of  $\text{CuCl}_2 \cdot 2\text{H}_2\text{O}$  powder in 20 mL of methanol. The 0.025 M  $\text{CoCl}_2 \cdot 6\text{H}_2\text{O}$  solution was prepared by dissolving 0.12 g of  $\text{CoCl}_2 \cdot 6\text{H}_2\text{O}$  powder in 20 mL of methanol. The 0.025 M  $\text{SnCl}_4 \cdot 5\text{H}_2\text{O}$  solution was prepared by dissolving 0.17 g of  $\text{SnCl}_4 \cdot 5\text{H}_2\text{O}$  powder in 20 mL of methanol. The appropriate amount of thiourea powder was dissolved in 20 mL of methanol, to achieve the ratio of cations to anions as 1:5 in the precursor solution. The molarity of thiourea was chosen in excess to avoid the loss of sulfur at elevated temperature [20]. The mixing of all the cationic solutions together in proper order resulted into brown colored solution with  $\text{pH} \approx 1$ . In this cationic solution, 20 mL of thiourea was added drop wise under vigorous stirring for 30 min. After addition of complete 20 mL thiourea to cationic solution, the final color of the precursor solution was observed to be dark blue with  $\text{pH} \approx 3$ . This solution was used for the deposition of CCTS thin films. To facilitate the regular deposition of thin films mechanized movement has been employed to spray nozzle at a frequency of 0.16 Hz. The atomization of precursor solution into fine spray droplets was carried out by

compressed filtered air with pressure kept at  $\approx 1$  bar. The 80 mL of precursor solution with a flow rate of 5 mL/min was sprayed onto soda lime glass (SLG) substrates which were preheated using temperature control arrangement. The working temperature range was chosen to be  $(\pm 2)^\circ\text{C}$  of threshold set point entered by user with the help of PID based logic in Arduino platform. The deposition temperature was chosen in the range 275–375  $^\circ\text{C}$  with an interval of 50  $^\circ\text{C}$ .

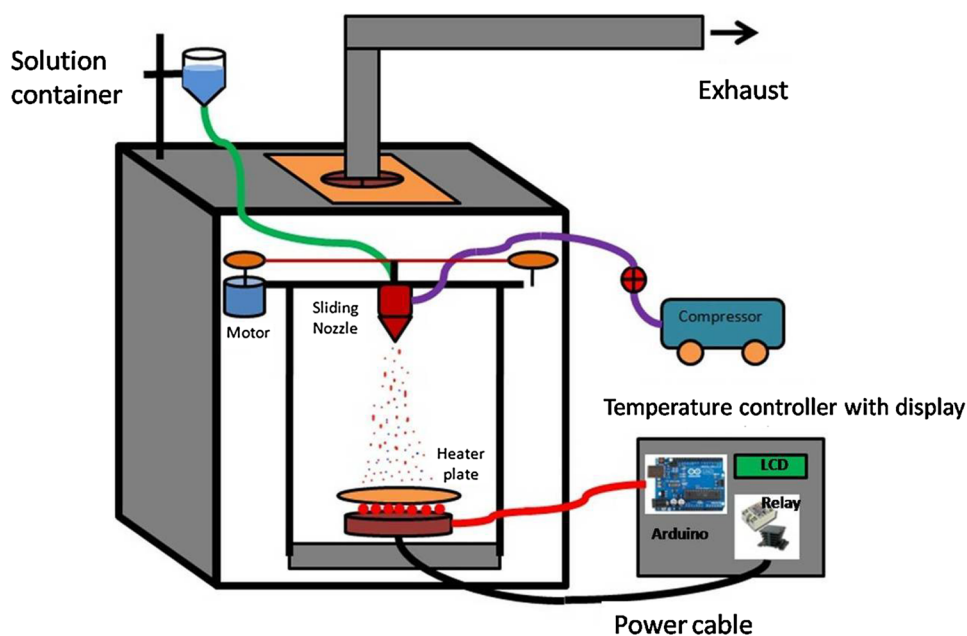
Surface profiler (Ambios, XP-I stylus profiler, USA) was used to carry out the thickness of measurement of the films. The structural properties of CCTS films were studied by using X-ray diffractometer (XRD) operated at 40 kV, 30 mA with  $\text{Cu K}_\alpha$  radiation ( $\lambda = 1.5406 \text{ \AA}$ ). The Raman analysis was carried out with the help of Renishaw inVia micro-Raman spectrometer at excitation wavelength of 633 nm of He–Ne laser as excitation source. The surface morphology of the films was studied by scanning electron microscopy (SEM) (JSM-6360, JEOL, Japan). The energy dispersive X-ray analysis (EDAX) of the film was recorded using EDX detector (Oxford Instruments, UK). UV–Visible spectrophotometer (UV 1800, Shimadzu, Japan) was used to record UV–visible absorbance spectra of the films.

## 3 Results and discussion

### 3.1 CCTS formation mechanism

The precursor solution for the formation of CCTS consists of dissolved metal chlorides and thiourea in methanol. The metal ions in the precursor solution attach to

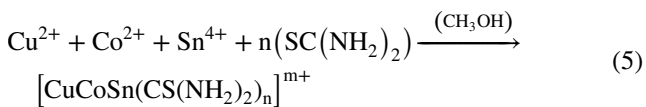
**Fig. 1** The schematic representation of spray pyrolysis unit used for deposition of CCTS thin films



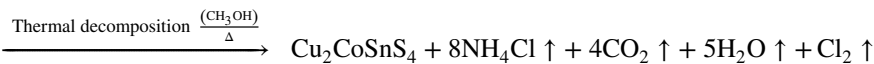
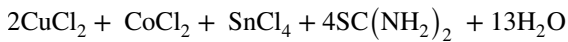
thiourea via sulfur atom to form metal–thiourea complex  $[\text{CuCoSn}(\text{CS}(\text{NH}_2)_2)_n]^{m+}$ . During spray pyrolysis heat treatment breaks the C–S bond present in the Cu–Co–Sn–thiourea complex, and metal sulfide i.e.  $\text{Cu}_2\text{CoSnS}_4$  is released [21–25]. The dissolutions of metal chlorides and thiourea in solvent will result into following reactions



The formation of metal–thiourea complex is represented by



The overall chemical reaction for CCTS formation on SLG substrates is given by



Thiourea used in the precursor solution not only acts as a source of sulfur but also it functions as reducing agent of divalent Cu ion to monovalent Cu ion [26].

### 3.2 Thickness measurement

The thickness of the CCTS films deposited at different substrate temperatures such as 275, 325 and 375 °C is found to be 527, 338 and 283 nm, respectively. The relatively larger value of thickness obtained at deposition temperature 275 °C is ascribed to incomplete thermal decomposition of spray droplets for the set temperature.

### 3.3 Structural analysis

Figure 2 shows XRD patterns of CCTS thin films deposited at different substrate temperatures. For the CCTS film deposited at substrate temperature of 275 °C, the intensity of (112) plane is weak as compared to film deposited at 325 °C. This may be due to insufficient thermal energy needed for decomposition of precursor solution. For the film deposited at substrate temperature of 325 °C, intensity of (112) plane is strong as well as the weak reflections at 2θ values of 47.50° and 56.40° are observed corresponding to (204) and (312) planes, respectively. This is due to the sufficient

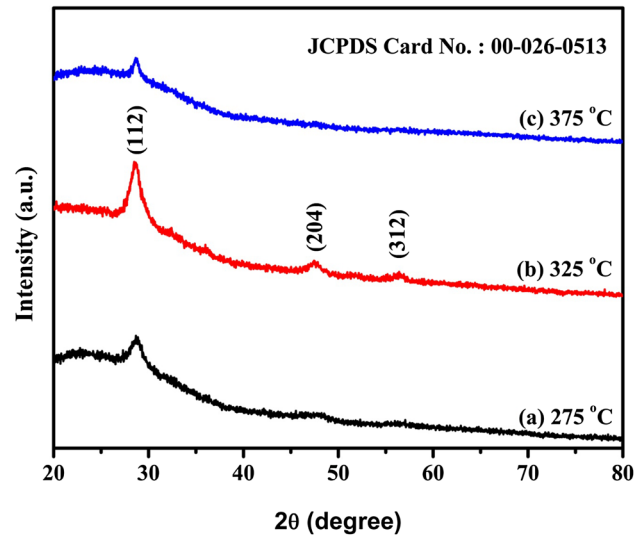


**Fig. 2** XRD patterns of CCTS films deposited at different substrate temperatures: (a) 275 °C, (b) 325 °C, (c) 375 °C

amount of thermal energy needed for thermal decomposition of precursor solution onto the glass substrates. Therefore,

this substrate temperature is suitable for optimum growth condition for film formation [27]. For the film deposited at substrate temperature of 375 °C, the intensity of (112) plane decreases and the reflections corresponding to (204) and (312) planes disappears. This is due to the complete decomposition of precursor solution in air before reaching towards the glass substrate, which results into the formation of less adherent powdery film onto the glass substrate. Also, at such a higher substrate temperature, less mass transport of precursor species onto glass substrate result into the decrease in film thickness [28].

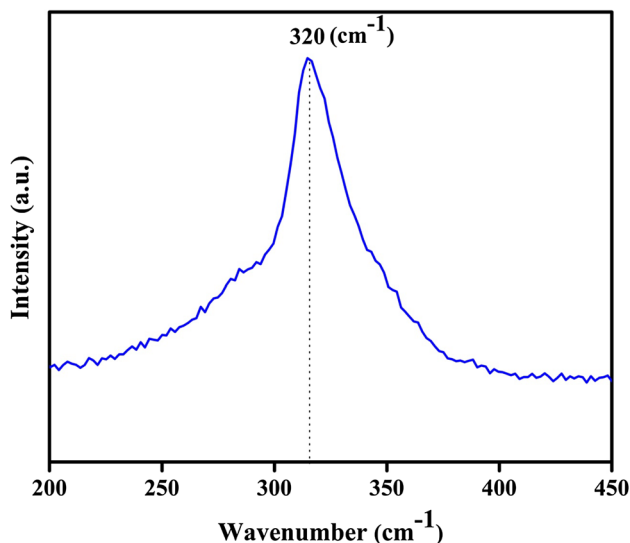
Comparing the XRD spectra of CCTS thin films to standard JCPDS Card No: 00-026-0513, it is confirmed that the spray deposited CCTS thin films exhibit stannite structure which has tetragonal unit cell. The average crystallite size (D) is calculated by Scherrer’s Eq. [29].

$$D = \frac{k\lambda}{\cos(\theta)} \quad (7)$$

where k is the shape factor, usually taken as 0.9 for spherical crystallites, λ is the wavelength of X-ray used, β is FWHM of the peak under consideration and θ is the Bragg’s angle. Table 1 shows the values of diffraction angle, interplanar spacing  $d_{hkl}$ , FWHM and crystallite size for (112) plane for

**Table 1** Structural parameters obtained for (112) plane for the CCTS films deposited at different substrate temperatures

Substrate temperature (°C)	Miller indices (hkl)	Standard diffraction angle (2θ)°	Observed diffraction angle (2θ)°	Standard d <sub>hkl</sub> (Å)	Calculated d <sub>hkl</sub> (Å)	FWHM(rad)	Crystallite size D (nm)
275	(112)	28.59	28.66	3.11	3.11	0.022	6.48
325			28.64			0.018	7.80
375			28.64			0.011	12.53

**Fig. 3** Raman spectrum of typical CCTS film deposited at 325 °C

the films deposited at different substrate temperatures. It is observed that with increase in substrate temperature from 275 to 375 °C, the full-width at half-maximum (FWHM) of (112) plane becomes narrower which represents the better crystallites formation in the CCTS films.

### 3.4 Raman analysis

XRD patterns of secondary phase like  $\text{Cu}_2\text{SnS}_3$  (CTS) and CCTS show close resemblance which limits the discrimination of CTS and CCTS structures by X-ray diffraction alone. Therefore, Raman analysis is carried out to confirm the phase purity of spray deposited CCTS thin films. Figure 3 shows a typical Raman spectrum for CCTS thin films deposited at 325 °C in the range of 200–450  $\text{cm}^{-1}$ . The most intense peak is observed at 320  $\text{cm}^{-1}$ , this can be allotted to the symmetry mode A1. It is mainly due to vibrations of S anions. The absence of peak at 350  $\text{cm}^{-1}$  denies the presence of metal polysulfide impurities of the types  $\text{SnS}_2$  and  $\text{CuCoS}_2$  in CCTS thin films [30].

### 3.5 Morphology of the films

Figure 4 put on view of SEM micrographs of CCTS thin films deposited at different substrate temperatures. At deposition temperature 275 °C morphology of the film is found to be nonuniform that represents the lack of distinct grains along with few voids over the surface. The grains in the films deposited at higher temperatures such as 325 and 375 °C, are appeared relatively larger than the grains seen in film at substrate temperatures 275 °C. For the films deposited at 325 °C the surface of the film seems to be flat with the evidence of voids over the film surface. As agglomeration is post nucleation process [31], the availability of nucleation centres resulted into large cauliflower like clusters at some region over the film surface. More compact morphology is observed for the films deposited at substrate temperatures 375 °C. The surface of the film is observed to be nonuniform which consists of some voids.

### 3.6 Compositional analysis

EDAX spectrum of the CCTS films deposited at temperature 325 °C is shown in Fig. 5. The Peaks corresponding to different constituent elements like Cu, Co, Sn, and S are clearly seen in the EDAX spectrum of the film. The composition ratio Cu:Co:Sn:S is found to be 2.13:1:1.91:5.39. EDAX spectrum reveals that the as deposited CCTS films are slightly Sn and S rich. The deviation from stoichiometry of the sulfur can be attributed to higher concentration of thiourea in the precursor solution.

### 3.7 Optical properties

The relation between absorption coefficient  $\alpha$  and incident photon energy  $h\nu$  is given by Eq. [32].

$$(\alpha h\nu) = A(h\nu - E_g)^n \quad (8)$$

where A is proportionality constant,  $E_g$  is optical band gap energy, n is an index representing the optical absorption process and it takes values equal to 1/2 or 2 for the direct and indirect allowed transitions respectively. As CCTS is direct band gap material, for direct allowed transitions n takes value equal to 1/2. The optical band gap of CCTS thin

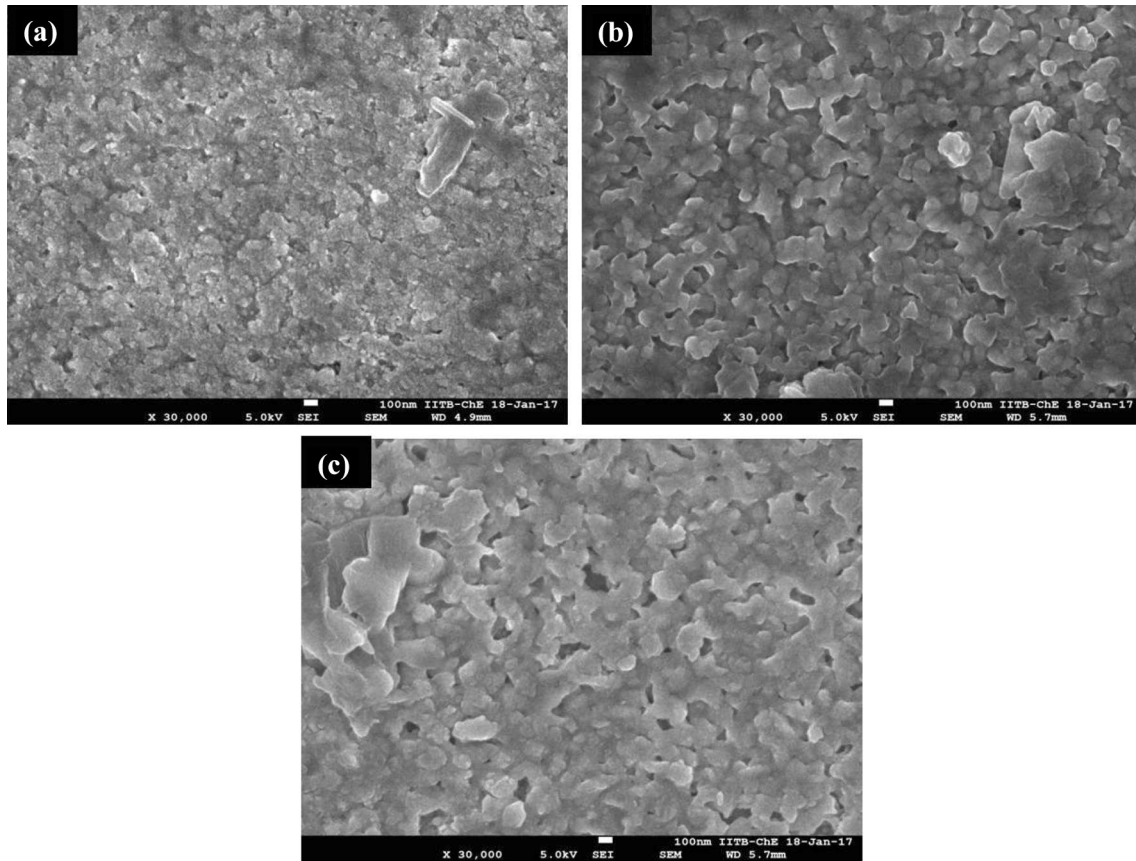


**Fig. 4** SEM micrographs with magnification of 30 kx of CCTS films deposited at different substrate temperatures: **a** 275 °C, **b** 325 °C, **c** 375 °C

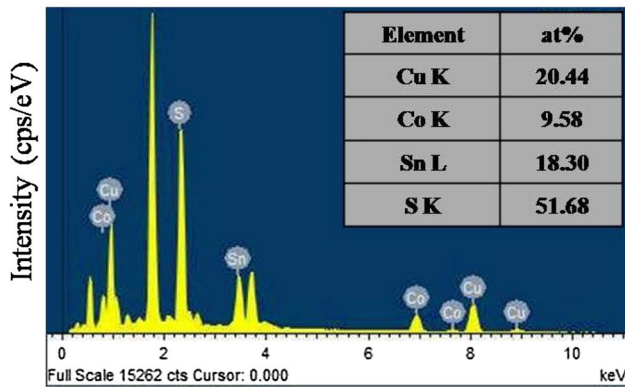


**Fig. 5** EDAX spectrum of the CCTS thin film deposited at substrate temperature 325 °C

films can be obtained by extrapolating the linear portion of the plots  $(\alpha h\nu)^2$  against  $h\nu$  at  $\alpha = 0$  as shown in Fig. 6. The energy band gap values of as deposited CCTS films are found to be decrease with increase in substrate temperature. The decrease in band gap values is ascribed to increase in crystallite size of the CCTS films deposited at different substrate temperatures [33, 34]. The energy band gap values of

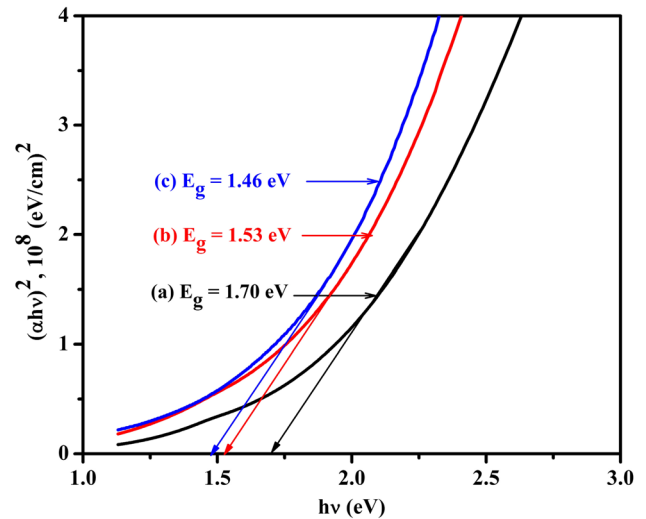


**Fig. 6** Plot of  $(\alpha h\nu)^2$  versus  $h\nu$  of CCTS films deposited at different substrate temperatures: (a) 275 °C, (b) 325 °C, (c) 375 °C

the CCTS films deposited at different substrate temperatures such as 275, 325 and 375 °C was found to be 1.70, 1.53 and 1.46 eV, respectively. The obtained band gap values for



CCTS films are quite close to the materials used for solar cell application [35].

## 4 Conclusions

Thin films of CCTS have been deposited by spray pyrolysis technique. The XRD studies revealed that the spray deposited thin films exhibit stannite structure with preferred orientation along (112) plane. The Raman analysis confirms the phase purity of spray deposited CCTS films, as the most intense peak is observed at  $320\text{ cm}^{-1}$  corresponding to A1 mode. The surface morphology study shows that the grains over the surface of the CCTS films become more distinct with increase in substrate temperature. The EDAX spectrum revealed the presence of elements Cu, Co, Sn and S. From the EDAX spectrum, it is observed that the elemental composition of CCTS films deposited at  $325\text{ }^{\circ}\text{C}$  is found to be Sn and S rich. The optical absorption study shows that the energy band gap values of as deposited films decrease with increase in substrate temperature. The spray deposited films at  $325\text{ }^{\circ}\text{C}$  have band gap close to optimal band gap of  $1.5\text{ eV}$  having compact and densely packed morphology, seems to be potential candidates for absorber layer in cost effective thin film solar cells.

**Acknowledgements** Authors wish to acknowledge “CENTRAL SURFACE ANALYTICAL FACILITY of IIT Bombay” for providing the SEM Images.

## References

1. F. López-Vergara, A. Galdámez, V. Manríquez, G. González, *Solid State Sci.* **49**, 54–60 (2015)
2. Y. Xie, C. Zhang, G. Yang, J. Yang, X. Zhou, J. Ma, *J. Alloys Compd.* **696**, 938–946 (2017)
3. W. Schfifer, R. Nitsche, *J. Appl. Phys.* **9**, 645–654 (1974)
4. A. Khare, B. Himmetoglu, M. Johnson, D.J. Norris, M. Cococcioni, E.S. Aydil, *J. Appl. Phys.* **111**, 083707 (2012)
5. C. An, K. Tang, G. Shen, C. Wang, L. Huang, Y. Qian, *Mater. Res. Bull.* **38**, 823–830 (2003)
6. Y. Cui, R. Deng, G. Wang, D. Pan, *J. Mater. Chem.* **22**, 23136–23140 (2012)
7. K. Mokurala, S. Mallick, P. Bhargava, *J. Power Sources* **305**, 134–143 (2016)
8. J.Y. Chane-Ching, a Gillorin, O. Zaberca, A. Balocchi, X. Marie, *Chem. Commun* **47**, 5229–5231 (2011)
9. B. Murali, M. Madhuri, S.B. Krupanidhi, *Cryst. Growth Des* **14**, 3685–3691 (2014)
10. A. Gupta, K. Mokurala, A. Kamble, S. Shankar, S. Mallick, P. Bhargava, *AIP Conf. Proc.* **1665**, 140022 (2015)
11. F. López-Vergara, A. Galdámez, V. Manríquez, P. Barahona, O. Peña, *J. Solid State Chem.* **198**, 386–391 (2013)
12. F. Ozel, *J. Alloys Compd.* **657**, 157–162 (2016)
13. F. Ozel, A. Yar, E. Aslan, E. Arkan, A. Aljabour, M. Can, I.H. Patir, M. Kus, M. Ersoz, *ChemNanoMat* **1** 477–481 (2015)
14. M.K. Gonc, E. Aslan, F. Ozel, I.H. Patir, *ChemSusChem* **9**, 600–605 (2016)
15. M. Benchikri, O. Zaberca, R. El Ouatib, B. Durand, F. Oftung, A. Balocchi, J.Y. Chane-Ching, *Mater. Lett.* **68**, 340–343 (2012)
16. O. Zaberca, A. Gillorin, B. Durand, J.Y. Chane-Ching, *J. Mater. Chem.* **21**, 6483 (2011)
17. L.D. Gulay, O.P. Nazarchuk, I.D. Olekseyuk, *J. Alloys Compd.* **377**, 306–311 (2004)
18. M. Quintero, E. Moreno, S. Alvarez, J. Marquina, C. Rincón, E. Quintero, P. Grima, J. Heano, M.A. Macías, *Rev. Lat. Met. Mater.* **4**, 28–38 (2014)
19. S.P. Desai, M.P. Suryawanshi, S.M. Bhosale, J.H. Kim, A.V. Moholkar, *Ceram. Int.* **41**, 4867–4873 (2015)
20. G. Ghosh, A. Biswas, A. Thangavel, R., and Udayabhanu, *RSC Adv* **6**, 96025–96034 (2016)
21. R.D. Angelo, C.L. Azanza Ricardo, A. Mittiga, P. Scardi, M. Leoni, *J. Sol–Gel Sci. Technol.* **72**, 490–495 (2014)
22. T.K. Chaudhuri, D. Tiwari, *Sol. Energy Mater. Sol. Cells* **101**, 46–50 (2012)
23. G. Rajesh, N. Muthukumarasamy, E.P. Subramaniam, S. Agilan, D. Velauthapillai, *J. Sol–Gel Sci. Technol.* **66**, 288–292 (2013)
24. S. Dias, B. Murali, S.B. Krupanidhi, *Mater. Chem. Phys.* **167**, 309–314 (2015)
25. Z. Seboui, A. Gassoumi, N. Kamoun-turki, *Mater. Sci. Semicond. Process.* **26**, 360–366 (2014)
26. S. Ikeda, M. Nonogaki, W. Septina, G. Gunawan, T. Harada, M. Matsumura, *Catal. Sci. Technol.* **3**, 1849–1854 (2013)
27. A. Kumar, P. Rajaram, *Mater. Sci. Eng. B.* **172**, 37–42 (2010)
28. A.A. Mane, M.P. Suryawanshi, J.H. Kim, A.V. Moholkar, *J. Colloid Interface Sci.* **483**, 220–231 (2016)
29. L. Shi, Y. Li, H. Zhu, Q. Li, *Chempluschem* **79**, 1638–1642 (2014)
30. F. López-Vergara, *J. Chil. Chem. Soc.* **4**, 2131–2135 (2013)
31. G. Nichols, S. Byard, M.J. Bloxham, J. Botterill, N.J. Dawson, A. Dennis, V. Diart, N.C. North, J.D. Sherwood, *J. Pharm. Sci.* **91**, 2103–2109 (2002)
32. B. Murali, S.B. Krupanidhi, *J. Appl. Phys.* **114**, 144312 (2013)
33. P.E. Agbo, *Adv. Appl. Sci. Res.* **3**, 599–604 (2012)
34. H.B. Lee, Y.M. Yoo, Y.H. Han, *Scr. Mater.* **55**, 1127–1129 (2006)
35. A. Ghosh, D.K. Chaudhary, A. Biswas, T. Rajalingam, G. Udayabhanu, *RSC Adv.* **6** 115204–115212 (2016)